1B.3 – THE DIFFUSIVE ROLE OF TURBULENCE IN AN INTENSE TROPICAL CYCLONE

Chibueze N. Oguejiofor[1*], George. H. Bryan[2], Richard Rotunno[2], Peter P. Sullivan[2], David H. Richter[1]

[1]University of Notre Dame

[2]NSF National Center for Atmospheric Research (NCAR)

1. INTRODUCTION

Accurate prediction of hurricane intensity continues to lag behind track prediction (DeMaria et al. 2014), partly due to the lack of sufficiently high resolution spatio-temporal observations of small scale processes within the hurricane boundary layer (HBL) (Emanuel 2017), defined roughly as the first kilometer above the surface in TCs. Incomplete representation of turbulence and its various parameterized roles in numerical weather models may be a substantial source of hurricane-intensity forecast error, especially in the short time range (e.g., rapid intensification events). This is partly because turbulent fluxes in the hurricane boundary layer, which are mostly parameterized using schemes developed for non-hurricane wind conditions (Chen et al. 2021), modulate enthalpy, moisture, and momentum exchange between the storm and the underlying ocean surface.

Flight level and ground-based observations of the near-eyewall region in intense hurricanes have alluded to the existence of organized turbulent structures in the hurricane boundary layer (Aberson et al. 2017). These structures, sometimes identified as coherent eddies, tornado-scale vortices or boundary-layer roll vortices based on their sizes, orientation, intensity, and proximity to the eyewall (Li and Pu 2023), can have important implications like modulating the severity of damage caused by hurricanes during landfall (Wurman and Kosiba 2018).

2. METHODOLOGY

Clearly, understanding the prevalence and role of these coherent turbulent structures in the hurricane eyewall is not only pertinent to research flight safety, but also to the understanding of heat, momentum and moisture flux which determines the bounds of storm intensity predictability.

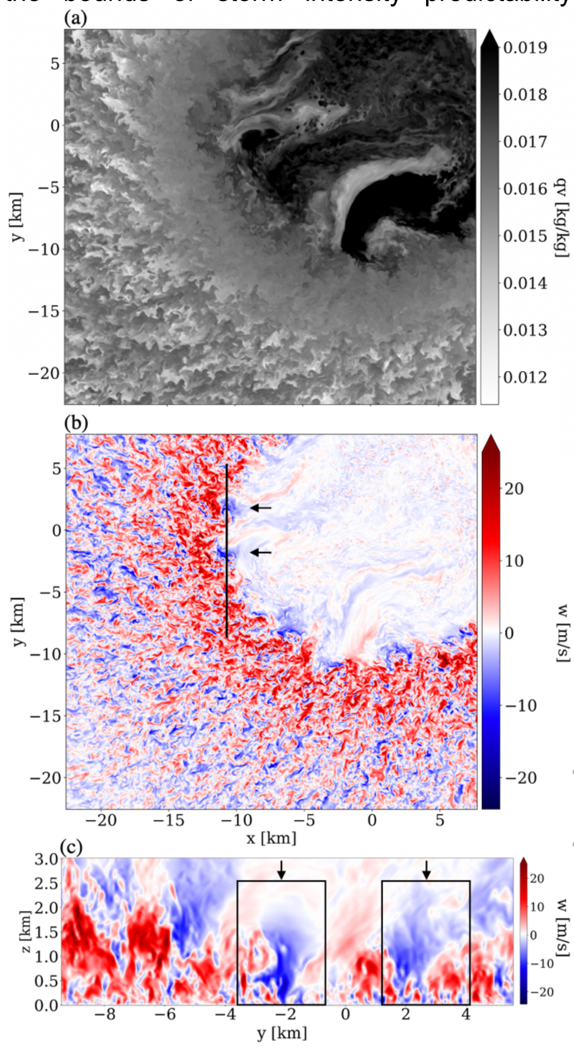

__Figure 1__: Windowed-in horizontal cross sections of (a) vertical velocity [m/s] in the southwest quadrant of the LES model domain and (b) water vapor mixing ratio [kg/kg], at z ≈700m. Vertical cross sections of (c) vertical velocity [m/s] in the inner eyewall (r≈11km). The black line in (a) represent the locations (inner eyewall) from which the vertical sections in (c) are plotted, respectively. The boxes in (c) highlight the vertical extent of two kilometer-scale intense downdraft features in (a).

---

* *Corresponding author address*: Chibueze N. Oguejiofor, 156 Fitzpatrick Hall, University of Notre Dame, Notre Dame, IN 46556; e-mail: coguejio@nd.edu

In the present study, LES of the inner core (i.e., eye, eyewall, and nearby rainbands) is utilized to characterize the behavior of coherent turbulent eddies responsible for vertical and horizontal fluxes within a simulated Category 5 hurricane (Fig. 1) and their role in the budget of the mean wind field.

Specifically, Cloud Model 1 (CM1) (Bryan and Fritsch 2002) was used to simulate an idealized Category 5 hurricane at turbulence- resolving horizontal and vertical grid intervals (Δx = Δy = 31.25m, Δz = 15.625m). The simulation, although idealized, was inspired by Hurricane Felix (2007), which was a Category 5 storm with a comparatively small RMW of about 11km (Aberson et al. 2017).

3. RESULTS

3.1 Mean Field Budget - The Role Of Turbulent Eddies

As shown above (Fig. 1), coherent turbulent velocity structures are prevalent in the TC boundary layer, particularly in the eyewall. The question thus arises as to what role they play in the budget of the mean wind field equations. Do they act to enhance momentum in the eyewall or do they act to weaken it? To clarify the role of turbulent eddies, we derive the azimuthally and time-averaged momentum equations [in cylindrical coordinates and compute each term appearing on the right hand side from the model simulation output:

$$\frac{\partial\langle u\rangle}{\partial t} = -\langle u\rangle\frac{\partial\langle u\rangle}{\partial r} - \langle w\rangle\frac{\partial\langle u\rangle}{\partial z} - \underbrace{\frac{1}{r}\frac{\partial}{\partial r}\langle ru'^2\rangle}_{T_r^u} - \underbrace{\frac{\partial}{\partial z}\langle u'w'\rangle}_{T_z^u}\cdots$$
$$+\frac{\langle v\rangle^2}{r} + \frac{\langle v'^2\rangle}{r} - \frac{\partial\langle\phi\rangle}{\partial r} + f\langle v\rangle + \langle F^u\rangle\ldots(1),$$

$$\frac{\partial\langle v\rangle}{\partial t} = -\langle u\rangle\frac{\partial\langle v\rangle}{\partial r} - \langle w\rangle\frac{\partial\langle v\rangle}{\partial z} - \underbrace{\frac{1}{r^2}\frac{\partial}{\partial r}\langle r^2u'v'\rangle}_{T_r^v} - \underbrace{\frac{\partial}{\partial z}\langle v'w'\rangle}_{T_z^v}\cdots$$
$$-\frac{\langle u\rangle\langle v\rangle}{r} - f\langle u\rangle + \langle F^v\rangle\ldots(2),$$

$$\frac{\partial\langle w\rangle}{\partial t} = -\langle u\rangle\frac{\partial\langle w\rangle}{\partial r} - \langle w\rangle\frac{\partial\langle w\rangle}{\partial z} - \underbrace{\frac{1}{r}\frac{\partial}{\partial r}\langle ru'w'\rangle}_{T_r^w} - \underbrace{\frac{\partial}{\partial z}\langle w'^2\rangle}_{T_z^w}\cdots$$
$$-\frac{\partial\langle\phi\rangle}{\partial z} + F_b + \langle F^w\rangle\ldots(3).$$

For the $\langle u\rangle$ budget in Eqn. (1), both radial and vertical eddy tendencies (Fig. 2) act to weaken the magnitude of the radial velocity in the inflow region. From Fig. 2a, the radial tendency field is a dipole at r≈11km, indicating diffusion of radial inflow along the strong gradient of $\langle u\rangle$. Furthermore, the vertical eddy-flux divergence (Fig. 2b) primarily acts to diminish the magnitude of radial inflow close to the surface (from the inflow BL to the corner flow), ultimately leading to the loss of momentum due to drag. A comparison of the radial and vertical eddy tendencies here indicate that the weakening role (red shading) of the vertical term is significantly larger, especially closer to the surface (below the height of maximum radial inflow).

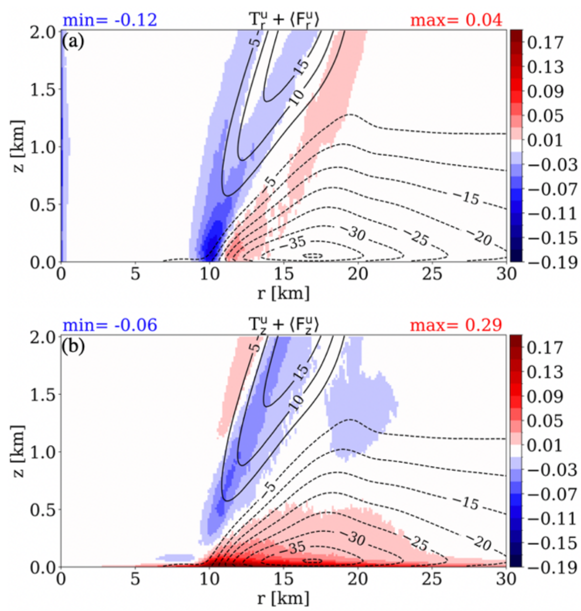

***Figure 2**: Contour plots of azimuthally and time-averaged radial velocity field $\langle u\rangle$, overlain with shadings from the contributions due to turbulent eddy tendencies in the (a) radial ($T_r{}^u$ in ms^{-2}) and (b) vertical ($T_z{}^u$ in ms^{-2}).*

For the ⟨v⟩ budget in Eqn. (2), because of the negative values of eddy tendencies in the vicinity of V_{max} (r≈11km), both the radial and vertical eddy tendencies act to weaken the maximum value of the tangential wind speed. In Fig. 3a, the radial eddy tendency is a dipole just inward of the eyewall (r≈10km), and thus acts to diffuse momentum at the eye/eyewall interface. The vertical eddy tendency (Fig. 3b) primarily diffuses momentum along and just inward of V_{max}. In addition, the vertical eddy tendency primarily acts to reduce momentum along most of near-surface boundary leading to the eyewall (weak blue shading in Fig. 3b outside of V_{max}).

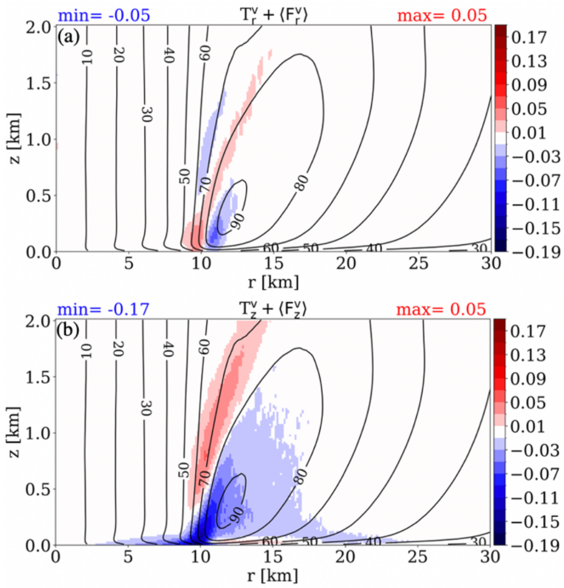

Figure 3*: Same as Fig. 3 but for tangential velocity ⟨v⟩.*

Finally, considering the $\langle w \rangle$ budget, Figs. 4a-b show the contribution of the radial and vertical eddy tendencies to the mean flow. The radial eddy tendency (Fig. 4a) is small compared to the vertical eddy tendency (Fig. 4b) which is negative in the lowest region of the inner eyewall.

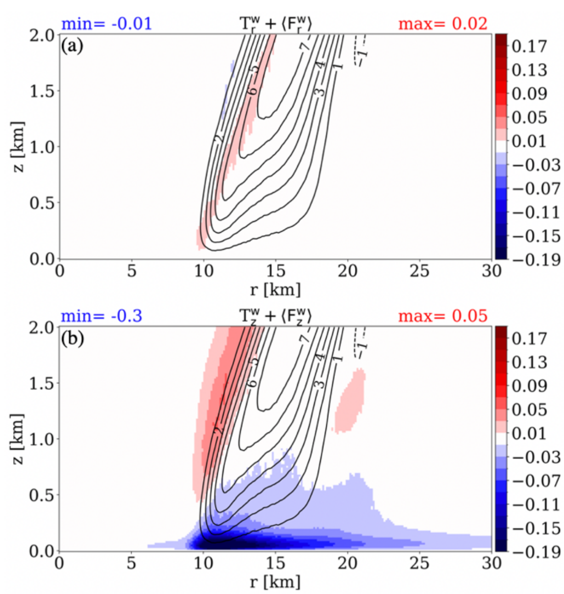

Figure 4*: Same as Fig. 3 but for vertical velocity ⟨w⟩.*

The vertical eddy tendency acts to diminish the strength of the mean upward flow of the vertical velocity in the eyewall. In other words, it opposes the mean eyewall updraft, reducing the magnitude of mean vertical velocity near the surface in the eyewall.

4. DISCUSSION

The foregoing analysis indicates that the net effect of the turbulent eddy tendencies in the eyewall region is essentially diffusive in nature – acting to reduce V_{max}, weaken the strength of the radial inflow close to the surface, as well as the upward flow of air in the eyewall.

5. REFERENCES

Aberson, S. D., J. A. Zhang, and K. N. Ocasio, 2017: An extreme event in the eyewall of Hurricane Felix on 2 September 2007. Monthly Weather Review, 145 (6), 2083–2092.

Bryan, G. H., and J. M. Fritsch, 2002: A benchmark simulation for moist nonhydrostatic numerical models. Monthly Weather Review, 130 (12), 2917–2928.

Chen, X., G. H. Bryan, J. A. Zhang, J. J. Cione, and F. D. Marks, 2021: A framework for simulating the tropical cyclone boundary layer using large-eddy simulation and its use in evaluating PBL parameterizations. Journal of the Atmospheric Sciences, 78 (11), 3559–3574.

DeMaria, M., C. R. Sampson, J. A. Knaff, and K. D. Musgrave, 2014: Is tropical cyclone intensity guidance improving? Bulletin of the American Meteorological Society, 95 (3), 387–398.

Emanuel, K., 2017: Will global warming make hurricane forecasting more difficult? Bulletin of the American Meteorological Society, 98 (3), 495–501.

Li, X., and Z. Pu, 2023: Dynamic Mechanisms Associated with the Structure and Evolution of Roll Vortices and Coherent Turbulence in the Hurricane Boundary Layer: A Large Eddy Simulation During the Landfall of Hurricane Harvey. Boundary-Layer Meteorology, 1–22.

Wurman, J., and K. Kosiba, 2018: The role of small-scale vortices in enhancing surface winds and damage in Hurricane Harvey (2017). Monthly Weather Review, 146 (3), 713–722.